



Design, synthesis, and characterization of the electrochemical, nonlinear optical properties, and theoretical studies of novel thienylpyrrole azo dyes bearing benzothiazole acceptor groups

M. Manuela M. Raposo^{a,*}, M. Cidália R. Castro^a, A. Maurício C. Fonseca^a, Peter Schellenberg^b, M. Belsley^b

^a Center of Chemistry, University of Minho, Campus of Gualtar, 4710-057 Braga, Portugal

^b Center of Physics, University of Minho, Campus de Gualtar, 4710-057 Braga, Portugal

ARTICLE INFO

Article history:

Received 4 March 2011

Received in revised form 9 May 2011

Accepted 11 May 2011

Available online 20 May 2011

Dedicated to the Centenary of the Portuguese Chemical Society

Keywords:

Heterocyclic azo dyes

Thienylpyrrole

Benzothiazole

Nonlinear optical (NLO) materials

Reverse polarity

First hyperpolarizability (β)

Thienylpyrroles as auxiliary donors

Redox properties

Density functional theory (DFT)

Thermal stability

ABSTRACT

Two series of related donor–acceptor conjugated heterocyclic azo dyes based on the thienylpyrrole system, functionalized with benzothiazol-2-yl (**5–6**) or benzothiazol-6-yl acceptor groups (**7**) through an N=N bridge, have been synthesized by azo coupling using 1-alkyl(aryl)thienylpyrroles (**1**) and benzothiazolyl diazonium salts (**2–4**) as coupling components. Their optical (linear and first hyperpolarizability), electrochemical, and thermal properties have been examined. Optimized ground-state molecular geometries and estimates of the lowest energy single electron vertical excitation energies in dioxane solutions were obtained using density functional theory (DFT) at the B3LYP/6-31+G(d,p) level. Hyper-Rayleigh scattering (HRS) in dioxane solutions using a fundamental wavelength of 1064 nm was employed to evaluate their second-order nonlinear optical properties. Of these systems, the benzothiazol-2-yl-diazenes **5–6** exhibit the largest first hyperpolarizabilities ($\beta=460\text{--}660\times 10^{-30}$ esu, T convention) compared to benzothiazol-6-yl-diazenes **7** ($\beta=360\text{--}485\times 10^{-30}$ esu, T convention). Good to excellent thermal stabilities were also obtained for all azo dyes (235–317 °C). This multidisciplinary study showed that modulation of the optical and electronic properties can be achieved by introduction of the benzothiazole acceptor group in the thienylpyrrole system through position 2 or 6 of the benzothiazole heterocycle.

© 2011 Elsevier Ltd. All rights reserved.

1. Introduction

Aryl and (hetero)aryl diazenes have long been used as dyes and colorants, but more recent applications have sought to exploit their use as versatile precursors in several organic reactions, the ability to photo switch the geometry and associated electronic and optical properties of these molecules for various applications including the fabrication of second harmonic generation chromophores, memories and switches,^{1,2} materials for organic solar cells,³ and chemosensors.⁴

Heterocycles by themselves can also play an important role as versatile building blocks in several areas of advanced materials chemistry, second-order nonlinear optical (NLO) applications being

an important example. It has been shown by theoretical and experimental studies, that the use of heteroaromatics, such as pyrrole, thiophene or (benzo)thiazole, in which electrons are more easily delocalizable compared to aryl derivatives, can lead to enhanced hyperpolarizabilities.^{5–7}

One of the major challenges in the design and optimization of the second-order polarizability of organic NLO materials consists in finding substituents with an optimal combination of their donor/or acceptor strength for a given parent chromophore. Although a large variety of donor, acceptor, and spacer groups have been used for the design of NLO chromophores, the use of strong donating moieties, such as electron-rich heteroaromatic rings has seldom appeared in the NLO literature.^{1a,7,8} Even rarer are examples of azo dyes bearing pyrrole or thienylpyrrole systems as donor moieties functionalized with aryl or heteroaryl diazene acceptor systems specifically designed for nonlinear optical and photochromic

* Corresponding author. Tel.: +351 253 604381; fax: +351 253 604382; e-mail address: mfox@quimica.uminho.pt (M.M.M. Raposo).

applications.^{1a,b,8a,8g} On the other hand, several investigators reported studies concerning the use of benzothiazole heterocycle as acceptor group in NLO chromophores.^{5b,6a–c,9}

Recently we have designed, synthesized, and characterized several series of donor–acceptor substituted π -conjugated systems in which we have used 1-alkyl(aryl)thienylpyrroles as donor moieties functionalized with several acceptor groups (dicyanovinyl, tricyanovinyl, benzothiazolyl, benzimidazolyl, aryldiazene, and thiazolyldiazene). Evaluation of the electrochemical and optical (linear and nonlinear) properties of these novel donor–acceptor systems revealed that they could be used as potential candidates for second-order NLO⁸ and photochromic applications.^{8g,10} Moreover, our experimental and theoretical results concerning the auxiliary donor/acceptor effect of electron-rich and electron-deficient heterocycles on push–pull thienylpyrrole π -conjugated systems have shown that the position of the acceptor groups, such as dicyanovinyl or electron-deficient heterocycles (e.g., benzothiazole or benzimidazole) on the thienylpyrrolyl system can have a clear influence on the electronic and optical properties of these heterocyclic chromophores.

In view of our recent results^{8,10} and other previous studies^{1a,4g,9d,9f} we decided to investigate the effect of different benzothiazole acceptor groups linked to the thienylpyrrole (**1**) donor system through an azo bridge on the electronic and optical properties of the novel heterocyclic azo dyes. Thus two novel series of azobenzothiazolyl thienylpyrroles **5–7** were designed, synthesized and their electrochemical and optical (linear and nonlinear) properties were evaluated.

The aim of the present work is to demonstrate that combined tuning of optical and electrochemical properties of heterocyclic azo derivatives **5** and **7** can be achieved by functionalization of the thienylpyrrole (**1**) systems with heteroaromatic benzothiazoles linked to the π -conjugated system/donor moiety through different positions of the benzothiazole ring (2 or 6). To this end, two series of structurally related chromophores have been designed and investigated. One is based on thienylpyrrolyl-benzothiazol-2-yl-diazenes **5–6** (normal polarity) and the other on thienylpyrrolyl-benzothiazol-6-yl-diazenes **7** (reverse polarity). The influence of the different regiochemistries of the heterocyclic acceptor group was investigated by combined experimental and theoretical studies of the electronic, linear, and nonlinear optical properties of these heterocyclic azo dyes.

In addition, the azo dyes **5** and **7** were compared to their similar thienylpyrrole derivatives functionalized with phenyldiazene **8a**,^{8g} thiazolyldiazene **9a–c**,^{8g} and benzothiazole **10a–b**^{8d} moieties (Fig. 1). First, the influence of an additional N=N bridge on the electronic and optical properties has been studied by comparing thienylpyrrolyl-benzothiazol-2-yl-diazenes **5** with the corresponding thienylpyrrolyl-benzothiazoles **10**.^{8d} Furthermore comparison of thienylpyrrolyl-thiazolyldiazenes **9a–c**^{8g} with compounds **5a–c** showed the higher acceptor capacity of the benzothiazole electro-deficient heterocycle when compared to the thiazole ring.

Second, the effect of the substitution of a phenylazo moiety by the heterocyclic benzothiazolyldiazene acceptor system have been studied by comparison of thienylpyrrolyl-benzothiazol-6-yl-diazene **7a** with **8a**^{8g} (Fig. 1).

2. Results and discussion

2.1. Synthesis

Usually push–pull benzothiazole derivatives reported in the literature have normal polarity,^{9a–c,9e,9g–q} with the exception of the three articles published recently by Hrobárik et al. concerning the theoretical studies^{9d,j} and the synthesis of a few examples of structurally simple benzothiazole derivatives having reverse polarity.^{9f} The reverse polarity of push–pull heterocyclic NLO chromophores are specially important when an additional electron-withdrawing group is attached to the benzothiazole ring. Additionally, as the strength of the withdrawing group substituted in the benzothiazole heterocycle is increased, the resulting increase in the NLO response becomes more sensitive to its position in the benzothiazole ring.

The effects of several molecular modifications were examined with the aim of understanding this structure–property relationship. The results^{9d,f,j} suggested that the most promising derivatives in terms of optimal NLO-phore properties (highest quadratic molecular hyperpolarizabilities) are benzothiazole derivatives containing acceptor groups on position 2 and a π -donor styryl or heteroalkenyl group in position 6 of the benzothiazole ring. Having in mind these theoretical studies and also our recent work⁸ we decide to synthesize two types of donor–acceptor benzothiazole derivatives with different dipole moment directions in order to evaluate the effect of different geometries of the benzothiazole dyes on their thermal, electrochemical, and optical properties: compounds with normal polarity in which the thiazole moiety is linked to the azo bridge through the C-2 of the heterocycle (**5–6**) and chromophores with reverse polarity^{9f} in which the benzothiazole heterocycle is linked to the azo bridge through C-6 (**7**).

Thienylpyrroles **1a–d**¹¹ have been used as coupling components together with benzothiazolyl diazonium salts **2–4** in order to prepare heterocyclic azo dyes **5–7** (Scheme 1). Therefore, diazotation of 2-aminobenzothiazole, 6-aminobenzothiazole, and 2-amino-6-methylbenzothiazole with NaNO₂ in HCl at 0–5 °C in water gave the corresponding diazonium salts **2–4**, which reacted immediately with thienylpyrroles **1a–d** in acetonitrile at 0 °C given benzothiazolyldiazenes **5–7** in fair to good yields (10–81%). Higher yields (60–81%) were obtained in the synthesis of thienylpyrrole azo dyes **7a–c** bearing the azo bridge substituted on position 6 of the benzothiazole heterocycle probably due to the higher stability of diazonium salt **4** when compared to **2**.

The structures of thienylpyrrolyl-benzothiazol-2-yl-diazenes **5–6** and thienylpyrrolyl-benzothiazol-6-yl-diazenes **7** were unambiguously confirmed by their analytical and spectral data.

2.2. Electronic structure analysis

The structures and charge transfer transitions of the heterocyclic azo dyes were first analyzed by ¹H NMR spectroscopy (Table 1) and cyclic voltammetry (Table 2).

For example in the ¹H NMR spectra of thienylpyrrole derivatives **5a–b** and **6a** functionalized with a benzothiazol-2-yl-diazene moiety on the 2-position of the pyrrole ring exhibit two

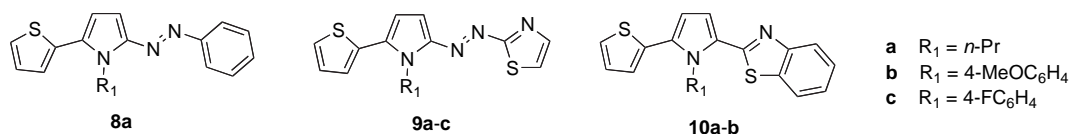
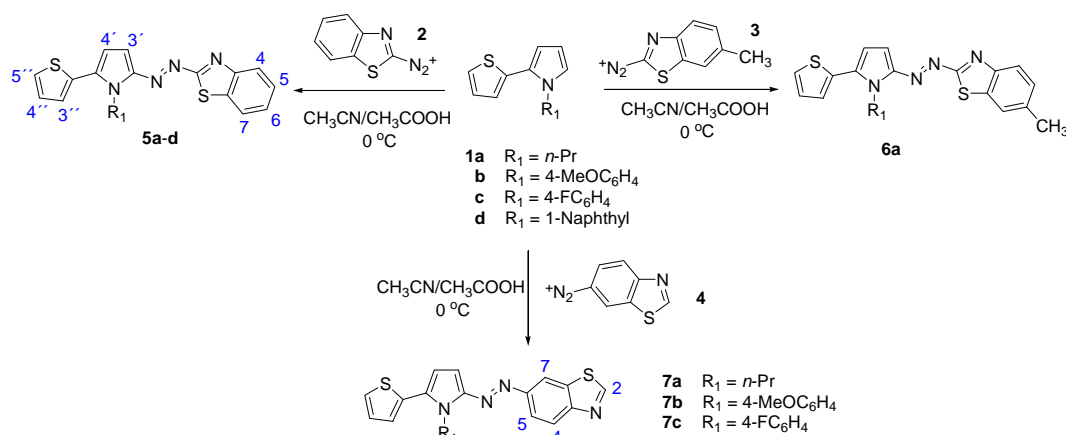


Fig. 1. Structure of thienylpyrrole derivatives **8a**, **9a–c**, and **10a–b**.^{8d,8g}



Scheme 1. Synthesis of benzothiazole azo dyes **5–7** through azo coupling reaction of thienylpyrroles **1** with benzothiazolyl diazonium salts **2–4**.

doublets at about 6.89–7.13 and 7.12–7.27 ppm were detected with coupling constants of 4.6–4.9 Hz indicating the presence of two adjacent protons (4'-H and 3'-H) at the corresponding pyrrole moiety. In the ^1H NMR spectra of thienylpyrrole azo dye **5d** four signals at about 7.51 (double triplet), 7.61 (double triplet), 7.84 (double doublet), and 7.90 (double doublet) were detected and were attributed, respectively, to the 5, 6, 4, and 7-H protons in the benzothiazole ring.

In the ^1H NMR spectrum of derivative **6a** bearing a 6-methylbenzothiazol-2-yl- moiety an additional singlet at 2.86 ppm was detected due to the methyl group attached to C6. Moreover, the signals attributed to the 5-H and 7-H in the benzothiazole system were detected as a double doublet at 7.35 ppm and as a doublet at 7.79 ppm, respectively, with coupling constants of 8.3 and 2.0 Hz for 5-H and 2.0 Hz for 7-H. On the other hand for thienylpyrrolyl-

benzothiazol-6-yl-diazenes **7** four signals were detected at about 8.07–8.18 (doublet), 7.76–8.06 (double doublet), 8.33–8.53 (doublet), and 9.30–9.31 (singlet). These signals were attributed, respectively, to the 4, 5, 7, and 2-H protons in the benzothiazole ring.

The ^1H NMR chemical shifts reflect a charge separation in the ground state, consequently the analysis of these data in donor–acceptor compounds bearing benzothiazole electron-deficient heterocycles, such as benzothiazolyldiazenes **5–7** also confirms their push–pull character with a significant intramolecular charge transfer (ICT) from the donor thienylpyrrole moiety to the acceptor benzothiazole groups (Table 1).¹² The effect of the substitution of a phenyl group for dye **8a** by a benzothiazole heterocycle (e.g., **5a**) is noteworthy. All the protons of the thienylpyrrole **5a** (3'-H and 4'-H, and 3'', 4'', and 5''-H) were shifted to higher chemical shifts (e.g., 4'-H and 3'-H δ =6.89 and 7.15 ppm,

Table 1
Chemical shifts of protons of the heterocyclic azo dyes **5–7**^a

Compd	R_1	4-H	5-H	6-H	7-H	3'-H	4'-H	3''-H	4''-H	5''-H
5a	<i>n</i> -Pr	7.99–8.02	7.46	7.54	7.99–8.02	7.15	6.89	7.61	7.32	7.79
5b	4-MeOC ₆ H ₄	7.90	7.40	7.45–7.54	7.96	7.27	7.13	7.29	7.08–7.14	7.56
5c	4-FC ₆ H ₄	7.90	7.41	7.45–7.52	7.96	7.27–7.29	7.13	7.27–7.29	7.10–7.13	7.59
5d	1-Naphthyl	7.84	7.51	7.61	7.90	7.40–7.43	7.32–7.34	7.25	6.96–6.98	7.40–7.43
6a	<i>n</i> -Pr	7.88	7.35	—	7.79	7.12	6.87	7.59	7.32	7.80
Compd	R_1	2-H	4-H	5-H	7-H	3'-H	4'-H	3''-H	4''-H	5''-H
7a	<i>n</i> -Pr	9.30	8.18	8.06	8.53	6.83	6.58	7.35	7.19–7.22	7.59
7b	4-MeOC ₆ H ₄	9.31	8.07	7.76	8.33	7.00–7.02	6.87	7.00–7.02	7.00–7.02	7.42–7.46
7c	4-FC ₆ H ₄	9.31	8.08	7.76	8.34	7.00	6.87	7.00–7.04	7.00–7.04	7.45

^a Proton NMR measurements carried out in deuterated acetone at 400 MHz, with chemical shift values in ppm. The numbering scheme of protons is shown in Scheme 1.

Table 2
Electrochemical data and theoretical values for the HOMO and LUMO energies for compounds **5–7**, **8a**, and **9a**

Compound	Reduction ^a			Oxidation ^a	HOMO DFT ^b	LUMO DFT ^b	Band gap (eV)	
	$-^1E_{1/2}$ (V)	$-^2E_{1/2}$ (V)	$-^3E_{1/2}$ (V)				Exp. ^c	Theory
5a	1.36	2.08	—	0.70	−5.6226	−3.0716	2.06	2.5510
5b	1.33	1.97	—	0.66	−5.7018	−3.1320	1.99	2.5698
5c	1.35	2.03	—	0.69	−5.7418	−3.1633	2.04	2.5785
5d	1.36	2.07	2.87	0.72	−5.7236	−3.1535	2.02	2.5701
6a	1.41	2.22	—	0.67	−5.5693	−3.0403	2.08	2.5290
7a	1.81	2.40	—	0.57	−5.6071	−2.6841	2.38	2.9230
7b	1.73	2.26	—	0.55	−5.5344	−2.7176	2.28	2.8168
7c	1.77	2.29	—	0.54	−5.5802	−2.7478	2.31	2.8324
8a ^{8g}	1.95	—	—	0.56	−5.4190	−2.5744	2.51	2.8426
9a ^{8g}	1.51	2.25	—	0.59	−5.5502	−2.9676	2.10	2.5826

^a Measurements made in dry dimethylformamide containing 1.0 mM of the indicated compound and 0.10 M [NBu₄][BF₄] as base electrolyte at a carbon working electrode with a scan rate of 0.1 V s^{−1}. All E values are quoted in volts versus the ferrocinium/ferrocene-couple. $E_{1/2}$ corresponds to the reversible process. E_{pa} correspond to the anodic peak potentials.

^b Calculated by DFT using B3LYP/6-31+G(d,p) in dimethylformamide.

^c $E_{HOMO} = -(4.39 + E_{pa})$ (eV) and $E_{LUMO} = -(^1E_{1/2} + 4.39)$ (eV).

respectively) when compared to the corresponding phenyldiazene azo dye **8a** (e.g., 4'-H and 3'-H δ =6.58 and 6.88 ppm, respectively)^{8g} indicating a decrease of the electron density due to the stronger electron-withdrawing power, a higher charge-demand c_x , of the benzothiazole ring, allowing a more efficient charge transfer from the donor to the acceptor group. On the other hand compounds **5** in which the electron-poor C-2 of the benzothiazole heterocycle is linked to the azo bridge, exhibit higher chemical shifts for all protons of the thienylpyrrole moiety (3'-H, 4'-H, 3''-H, 4''-H, and 5''-H) compared to derivatives **7** in which the benzothiazole heterocycle is linked to the azo bridge through position 6 indicating a more efficient charge transfer from the donor to the acceptor in compounds **5**. A possible explanation for these results is that in compounds **5** the electron-poor C2 of the 1,3-heteroaromatic thiazole moiety is at the acceptor end of the chromophore corresponding to the 'matched' configuration in which the electron-poor C2 is at the acceptor end of the molecule.

The 'matched' and 'un-matched' configurations of the 1,3-thiazole moiety are defined by the relative orientations between dipoles of thiazole and the NLO chromophore as a whole.

Table 2 displays the redox potentials measured in [NBu₄][BF₄]/DMF (1 mmol dm⁻³) by cyclic voltammetry, the theoretical values for the HOMO and LUMO energies calculated by DFT B3LYP/6-31+G(d,p) in DMF and the corresponding band gap values for compounds (**5a–d**, **6a**, **7a–c**, **8a**, and **9a**).

All molecules showed a donor–acceptor character with reversible reduction and irreversible oxidation processes. The irreversible oxidation process is associated with the oxidation of the pyrrole moiety. These results are consistent with previous electrochemical studies of other pyrrole and thiophenes derivatives.^{8a–c,13} In contrast all thienylpyrrole azo dyes (**5a–d** and **6a** and **7a–c**) bearing a benzothiazole acceptor group linked to the azo bridge through positions 2 (**5a–d** and **6a**) or 6 (**7a–c**) exhibited two monoelectronic reversible reductions indicating a high electron affinity of the chromophores. Compound **5d** shows a third reduction process attributed to the naphthyl group.¹⁴ The one-electron stoichiometry for these reduction processes is ascertained by comparing the current heights with known one-electron redox processes under identical conditions.^{8a} For all compounds, the two reduction processes are associated with the reduction of the (hetero)aromatic azo moiety. For all azo dyes it was also observed that the reduction potential values of the first process are only slightly influenced by the substituent on the nitrogen atom of the pyrrole ring. On the other hand the introduction of a benzothiazole acceptor group linked to the azo bridge through position 2 (compounds **5** and **6**) could significantly decrease the reduction potentials while increasing the oxidation potentials, when compared to derivatives **7** (bearing the benzothiazole heterocycle linked through the 6-position, e.g., **7b** $E_{1/2}$ =−1.73 V and **5b** $E_{1/2}$ =−1.33 V, (Fig. 2) and **5a** E_{pa} =0.70 V and **7a** E_{pa} =0.57 V suggesting a stronger electron-accepting ability of compounds **5**. At this moment two other comparisons can also be made between compound **7a** with aryldiazene **8a** or between benzothiazole azo dye **5a** with the corresponding thiazolyldiazene **9a**. The substitution of an aryldiazene system (**8a**) by the benzothiazol-6-yl- moiety (**7a**) or the substitution of a thiazole heterocycle (**9a**) by a benzothiazol-2-yl acceptor group (**5a**) results in a decrease of the reduction potentials (e.g., $E_{1/2}$ =−1.51 V for **9a** and $E_{1/2}$ =−1.36 V for **5a**) that could also be due to the stronger electron-accepting ability of compounds **5a** and **7a** compared, respectively, to **9a** and **8a**. These results are in agreement with the previous ¹H NMR analysis that showed increased electron densities for azo dyes **7** and **9a** and decreased electron densities for compounds **5**.

The electrochemical band gaps were calculated as described previously¹⁵ from the potentials of the anodic (oxidation of the thienylpyrrole) and cathodic processes (Table 2). Smaller band gaps were obtained for compounds **5** and **6** compared to azo dyes **7**.

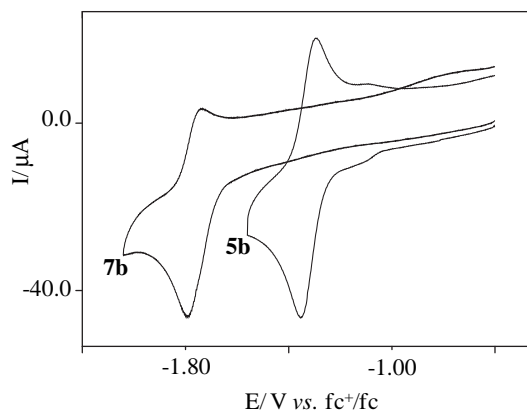


Fig. 2. Cyclic voltammograms for the first reduction step of compound **5b** and **7b** (1.0×10^{-3} mol dm⁻³) in DMF, 0.1 mol dm⁻³ [NBu₄][BF₄] at a vitreous carbon electrode, between −0.6 V and −2.10 V versus fc^+/fc , scan rate 0.1 V s⁻¹.

The efficient donor–acceptor conjugation leads to a lowering of the HOMO and the LUMO levels in **5** and **6**, revealing more efficient coupling between the thienylpyrrole system and the benzothiazole-2-yl acceptor. In contrast, a weaker donor–acceptor coupling of the benzothiazole-6-yl moiety **7** brings about an elevation of the HOMO and the LUMO levels. It is notable that the elevation of the HOMOs in comparable compounds of set **7** are around 0.1 eV, the elevation of the LUMOs is much stronger with elevations around 0.4–0.5 eV. Accordingly the contribution to the larger band gap in set **7** compared to set **5** is mostly due to the influence on the LUMOs. These observations are endorsed by the theoretical DFT analysis of the data, which show the same tendency. It is notable that the theoretical values for all compounds, the LUMOs are only slightly lower in energy compared to experiment (~ 0.1 eV), while the values for the HOMOs are lower by ~ 0.5 – 0.6 eV. This indicates a possible overestimation of conjugation and accordingly an underestimation of the charge separation in the HOMO.

2.3. Optical properties

Benzothiazolyl azo dyes **5–7** showed good solubility in common polar and non-polar organic solvents, such as dioxane, diethyl ether, ethanol, DMF, and DMSO. The extinction coefficients (ϵ) and the wavelength maxima λ_{max} of compounds **5–7** in several solvents, are summarized in Table 3 and were compared with the π^* values for each solvent, as determined by Kamlet and Taft.¹⁶ All chromophores exhibit broad and intense CT absorptions in the visible region from 452 nm to 509 nm in dioxane solutions. The *N*-aryl substituted chromophores **5b–d** exhibited a small red-shifted λ_{max} (7–8 nm) relative to the *N*-alkyl derivative **5a** suggesting a higher donor strength of aryl derivatives than the alkyl functionalized compound. On the other hand, the position of the linkage of the benzothiazolyl group to the azo bridge has significant effect on the electronic absorption property of NLO chromophores. For example, the 'matched' thiazole-based compounds **5a–d** exhibited a distinctively red-shifted λ_{max} (46–50 nm) with respect to the 'un-matched' derivatives **7a–c**. These results agree with the band gap calculations based on the redox properties (Table 2), which show increased band gaps for benzothiazol-6-yl azo dyes **7a–c** and decreased band gaps for benzothiazol-2-yl based compounds **5a–d**.

All the benzothiazole azo dyes exhibited positive solvatochromism ($\Delta\nu_{max}$ =855–1332 cm⁻¹) from diethyl ether to DMSO, suggesting the good optical nonlinearities of these chromophores (Table 3).¹⁷

The molecular first hyperpolarizabilities β of heterocyclic diazenes **5–7** were measured by Hyper-Rayleigh scattering (HRS) method¹⁸ at a fundamental wavelength of 1064 nm of a laser beam. Dioxane was

Table 3Solvatochromic data for thienylpyrrole **5–7** in five solvents with π^* values by Kamlet and Taft¹⁶

Azo dye	Diethyl ether (0.54) λ_{\max} (nm)	Ethanol (0.54) λ_{\max} (nm)	1,4-Dioxane (0.55) λ_{\max} (nm)	DMF (0.88) λ_{\max} (nm)	DMSO (1.00) λ_{\max} (nm)	$\Delta\nu_{\max}^a$ (cm ⁻¹)	ϵ (Dioxane) (M ⁻¹ cm ⁻¹)
5a	491	509	500	511	519	1099	(35,400)
5b	500	519	509	523	530	1132	(35,780)
5c	496	517	507	518	526	1132	(42,800)
5d	498	518	508	523	528	1141	(28,320)
6a	494	504	503	512	520	1013	(30,060)
7a	437	455	451	460	464	1332	(26,800)
7b	450	464	461	469	474	855	(21,900)
7c	445	458	452	465	468	1105	(36,130)

^a $\Delta\nu_{\max} = \nu_{\max}(\text{diethyl ether}) - \nu_{\max}(\text{DMSO})/\text{cm}^{-1}$.

used as the solvent, and the β values were measured against a reference solution of *p*-nitroaniline (pNA)¹⁹ in order to obtain quantitative values, while care was taken to properly account for possible fluorescence of the dyes (see [Experimental section](#) for more details). The static hyperpolarizability β_0 values²⁰ were calculated using a very simple two-level model neglecting damping. They are therefore only indicative and should be treated with caution ([Table 4](#)).

have the ‘matched’ orientation of the dipole moment with relevant substitution pattern.^{6c,9d,21}

At this stage, several comparisons could also be made between the nonlinear optical data of the new benzothiazole azo dyes **5** and **7**, with thienylpyrrole derivatives functionalized with aryl diazene moiety **8a**,^{8g} thiazolyldiazene **9a–c**^{8g} or benzothiazole heterocycles **10a–b**,^{8d} recently reported by us ([Fig. 1](#)). The results obtained

Table 4UV–vis absorptions, β and β_0 values and T_d data for benzothiazolyl azo dyes **5–7**^a and aryl and thiazolyl azo dyes **8–10**^{8d,8g}

Azo dye	λ_{\max} (nm)	β^b (10 ⁻³⁰ esu)	β_0^c (10 ⁻³⁰ esu)	T_d^d (°C)	Azo dye	λ_{\max} (nm)	β^b (10 ⁻³⁰ esu)	β_0^c (10 ⁻³⁰ esu)
5a	500	590	54	235	8a	419	225 ^f	72
5b	509	460	33	250	9a	486	390 ^f	51
5c	507	660	47	244	9b	493	370 ^f	41
5d	508	575	39	242	9c	491	470 ^f	55
6a	503	590	50	241	10a	353	150 ^f	74
7a	451	385	86	— ^e	10b	366	200 ^f	93
7b	461	485	95	317	—	—	—	—
7c	452	360	82	274	—	—	—	—
pNA	352	40 ¹⁹	20	—	—	—	—	—

^a Experimental hyperpolarizabilities and spectroscopic data measured in dioxane solutions.^b All the compounds are transparent at the 1064 nm fundamental wavelength. Values are reported in the T convention assuming a single longitudinal element dominates the hyperpolarizability tensor. Estimated uncertainties are 10% of the reported values.^c Data corrected for resonance enhancement at 532 nm using the two-level model with $\beta_0 = \beta [1 - (\lambda_{\max}/1064)^2] / [1 - (\lambda_{\max}/532)^2]$; damping factors not included 1064 nm.²⁰^d Decomposition temperature (T_d) measured at a heating rate of 20 °C min⁻¹ under a nitrogen atmosphere, obtained by TGA, corresponding to 5% of the decomposition of the material.^e Compound **7a** was obtained as an oil.^f Values rescaled from those reported in Ref. ^{8d,8g} to conform to the T convention and to take into account the most recent calibration from Ref. ¹⁹.

From [Table 4](#) it can be seen that the β values for azo dyes **5a–c** bearing the benzothiazol-2-yl group linked to the azo bridge exhibit higher first hyperpolarizabilities ($\beta=460\text{--}660\times 10^{-30}$ esu) compared to their benzothiazol-6-yl counterparts **7a–c** ($\beta=360\text{--}485\times 10^{-30}$ esu) showing that the β values are clearly influenced by the position of substitution of the benzothiazole heterocycle to the donor moiety through the azo bridge. However the extrapolation to zero frequency suggests that these gains are primarily due to the red shift of the HOMO–LUMO transition and that in fact the extrapolated static hyperpolarizabilities exhibit a trend in the opposite direction favoring the mismatched compounds. It is important to note that this extrapolation is based on a simple two-level model without damping effects and should be treated with some caution. One means of investigating this discrepancy would be to carry out detailed experimental measurements as a function of the incident wavelength over a wide spectral range to reliably extrapolate to static β values, but this is beyond our present capabilities. Previous theoretical studies have indicated that the relative orientation of the heteroaromatic rings (HR) on the molecular hyperpolarizability can be interpreted in terms of the dipole orientation and the substitution pattern in D–HR–A systems. Largest β values are predicted for all systems when they

showed that the substitution of a benzene ring (**8a**) by the electron-poor benzothiazol-6-yl group (**7a**) in the diazene moiety, maintaining the same thienylpyrrole donor system produced a bathochromic shift on the absorption wavelength maxima and a larger value of the molecular hyperpolarizability β (**8a**, $\lambda_{\max}=419$ nm, $\beta=225\times 10^{-30}$ esu and **7a**, $\lambda_{\max}=451$ nm, $\beta=385\times 10^{-30}$ esu). Due to the electron density deficiency on the ring C atoms, the benzothiazole heterocycle acts as electron-withdrawing group and also as an auxiliary acceptor. Furthermore, the large electronegativity and the lone electron pairs of S and N atoms in the thiazole moiety together with the extension of the conjugation length of the π -electron bridge also lead to an increase in the molecular hyperpolarizability. On the other hand substitution of a thiazol-2-yl diazene moiety **9a–c**, ($\beta=370\text{--}470\times 10^{-30}$ esu)^{8g} by the benzothiazol-2-yl diazene system **5a–c** while maintaining the same donor thienylpyrrole moieties leads to larger nonlinearities for compounds **5a–c**, ($\beta=460\text{--}660\times 10^{-30}$ esu) probably due to the more extensive electron delocalization (see the theoretically estimated oscillator strengths below) and red shift of the HOMO–LUMO energy gap. Noteworthy is also the effect of the introduction of an N=N bridge in benzothiazole azo dyes **5a–b** ($\beta=460\text{--}590\times 10^{-30}$ esu) compared to benzothiazoles **10a–b** ($\beta=150\text{--}200\times 10^{-30}$ esu).^{8d}

2.4. Theoretical calculations

Optimized ground-state molecular geometries and HOMO–LUMO gaps have been calculated using the Gaussian 09 program²² employing density functional theory using the B3LYP functional and the 6-31+G(d,p) basis set both on isolated molecules in vacuum and in dioxane and DMF solutions. For the latter, the Polarizable Continuum Model (PCM) using the integral equation formalism variant (IEFPCM) is used, which is the default in Gaussian 09.

Using the calculated geometry, time dependent DFT calculations employing the same functional and the same basis set (option: $\text{td}=(\text{nstates}=6)$) were then carried out to determine the vertical electronic transition energies. The results are summarized in Table 5 and compared with the experimentally determined values from the linear absorption measurements.

Table 5
Theoretical results for the energy, corresponding wavelength and oscillator strength of the lowest singlet transition for azo dyes 5–9

Azo dye	Predicted vertical transitions ^a			λ_{max} (nm) ^b
	energy (eV)	λ (nm)	f-value ^c	
5a	2.4224	511.83	1.5077	500
5b	2.4413	507.87	1.3742	509
5c	2.4442	507.27	1.3772	507
5d	2.4451	507.07	1.3764	508
6a	2.3949	517.70	1.5691	503
7a	2.6555	466.90	1.4342	451
7b	2.5929	478.17	1.1509	461
7c	2.6087	475.26	1.2266	452
8a	2.6556	466.88	1.2615	419
9a	2.4751	500.93	1.1966	486
9b	2.4956	496.82	1.0715	493
9c	2.5023	495.49	1.0813	491

^a Theoretically predicted values for the vertical transitions in dioxane solutions.

^b Observed wavelength of the linear absorption maximum.

^c Oscillator strength of the transition.

Overall the agreement between the theoretically predicted transition wavelengths and the experimentally determined absorption maxima is quite good. Slight exceptions are the diazenes functionalized with the *n*-propyl group in position 1 of the pyrrole ring (**5a**, **6a**, **7a**, **8a**, and **9a**) and the mismatched chromophores (**7a–c**) for which the theoretical calculations tend to predict bathochromic shifts that are about 2% greater than those that are observed experimentally.

The trends in the theoretical oscillator strengths are consistent with the above observations concerning the measured hyperpolarizabilities and suggest that a large part of the variation in the hyperpolarizabilities can be attributed to the differences in the amount of charge that participates in the ground state to first excited state vertical transition. The ‘matched’ azo dyes **5a–c** bearing the benzothiazol-2-yl group linked to the azo bridge possess stronger charge transfer transitions compared to their ‘mismatched’ benzothiazol-6-yl analogs **7a–c**, the oscillator strengths of the matched compounds being 5–10% greater than those of the respective mismatched molecules. The substitution of a benzene ring (**8a**) by the electron-poor benzothiazol-6-yl group (**7a**) in the diazene moiety increases the oscillator strength by just over 13% indicating a significant increase in the amount of charge that participates in the transition. Even more pronounced is the increase in oscillator strength by over 25% when the thiazol-2-yl diazene moiety (**9a–c**) is substituted by the benzothiazol-2-yl diazene system (**5a–c**), suggesting that the benzene ring contributes significantly to enhance the charge mobility of these molecules.

Figs. 3–5, below, display some of the obtained optimized lowest lying singlet state molecular geometries for azo dyes **5a–c**, **6a**, and **7a–b**, in dioxane. Only azo dyes **5a** and **6a** (Fig. 3), are strictly planar in the ground state, all other chromophores display some out of plane twisting see, for example, Fig. 4 (**5b–c**) and Fig. 5 (**7a–b**). It is noteworthy that azo dyes **5a** and **6a** also display some of the largest oscillator strengths and hyperpolarizabilities. In this regard azo dye **7a** (Fig. 5) is especially interesting when compared to **5a** (Fig. 3).

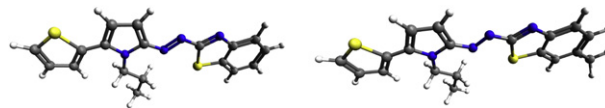


Fig. 3. Ground-state molecular structures for azo dyes **5a** (left) and **6a** (right) optimized using B3LYP/6-31+G(d,p).

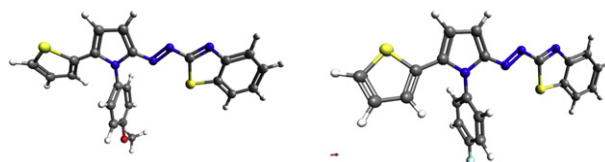


Fig. 4. Ground-state molecular structures for azo dyes **5b** (left) and **5c** (right) optimized using B3LYP/6-31+G(d,p).

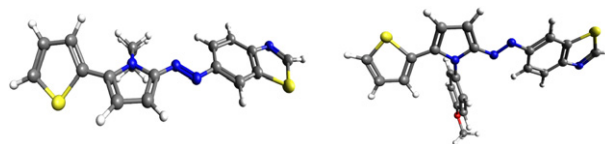


Fig. 5. Ground-state molecular structures for azo dyes **7a** (left) and **7b** (right) optimized using B3LYP/6-31+G(d,p).

2.5. Thermal properties of benzothiazole diazenes 5–7

The thermal stabilities of azo dyes **5–7** were evaluated by thermogravimetric analysis (TGA) under a nitrogen atmosphere, measured at a heating rate of 20 °C min^{−1}. As shown in Table 4 all compounds exhibit good to excellent thermal stability with decomposition temperatures varying from 235 to 317 °C. Benzothiazol-2-yl azo dyes **5a–d** and **6a** decompose between 235 and 250 °C, while benzothiazol-6-yl azo dyes **7b–c** showed an improved thermal stability by ca. 30–67 °C compared to the corresponding azo dyes **5b–c**. In addition, the electronic nature of the substituents on position 1 of the thienylpyrrole azo dyes **5a–d** and **7b–c** have some influence on their thermal stability being higher for derivatives substituted by the 4-methoxyphenyl group (e.g., **5b**, $T_d=250$ °C and **7b**, $T_d=317$ °C) (Table 4).

3. Conclusions

In conclusion we have developed two new series of benzothiazolyl-thienylpyrrole azo dyes with normal or with reverse polarity. By varying the position of linkage of the benzothiazole heterocycle (2 or 6) to the azo bridge, the electrochemical properties as well as the linear and nonlinear optical properties of this well-defined asymmetric push–pull π -conjugated systems can be readily tuned.

Theoretical calculations indicate that significant variations in the oscillator strength of the ground state–first excited vertical

transitions are associated with these changes. Experimental Hyper-Rayleigh scattering measurements report good β values for these benzothiazolyl-thienylpyrrole azo dyes with the best values obtained for the matched chromophores **5**.

4. Experimental

4.1. Materials

2-Amino-benzothiazole, 6-methyl-2-amino-benzothiazole, and 6-amino-benzothiazole used as precursors for the synthesis of benzothiazolyl-diazonium salts **2–4** were purchased from Aldrich and Fluka and used as received.

The synthesis of 1-propyl-thienylpyrrole **1a**^{11b} and 1-aryl-thienylpyrroles **1b–d**^{11a} was described elsewhere. TLC analyses were carried out on 0.25 mm thick precoated silica plates (Merck Fertigplatten Kieselgel 60 F₂₅₄) and spots were visualized under UV light. Chromatography on silica gel was carried out on Merck Kieselgel (230–240 mesh).

4.2. Synthesis

General procedure for the azo coupling of thienylpyrroles **1** with benzothiazolyl diazonium salts **2–4** to afford azo dyes **5a–d**, **6a**, and **7a–c**.

4.2.1. Diazotation of 2-amino-benzothiazole, 6-methyl-2-amino-benzothiazole, and 6-amino-benzothiazole. Heteroaromatic amines (1.0 mmol) were dissolved in HCl 6 N (1 mL) at 0–5 °C. A mixture of NaNO₂ (1.0 mmol) in water (2 mL) was slowly added to the well-stirred mixture of the thiazole solution at 0–5 °C. The reaction mixture was stirred for 20 min.

4.2.2. Coupling reaction with thienylpyrroles 1. The diazonium salt solution previously prepared (1.0 mmol) was added drop wise to the solution of thienylpyrroles **1** (0.52 mmol) and 2–3 drops of acetic acid in acetonitrile (10 mL). The combined solution was maintained at 0 °C for 1 h–2 h while stirred and diluted with chloroform (20 mL), washed with water and dried with anhydrous MgSO₄. The dried solution was evaporated and the remaining azo dyes were purified by column chromatography on silica with dichloromethane/*n*-hexane as eluent.

4.2.3. 2-(Benzo[d]thiazol-2-yl)-1-(1-(propyl)-5-(thiophen-2-yl)-1H-pyrrol-2-yl)-diazene 5a. Dark pink solid (86 mg, 47%) Mp 109–111 °C. ¹H NMR (acetone-*d*₆) δ 1.04 (t, *J*=7.2 Hz, 3H, CH₃), 1.93–1.99 (m, 2H, CH₂), 4.62 (t, *J*=7.2 Hz, 2H, NCH₂), 6.89 (d, 1H, *J*=4.6 Hz, 4'-H), 7.15 (d, 1H, *J*=4.6 Hz, 3'-H), 7.32 (m, 4''-H), 7.46 (dt, 1H, *J*=7.7 and *J*=1.2 Hz, 5-H), 7.54 (dt, 1H, *J*=7.7 and *J*=1.2 Hz, 6-H), 7.61 (dd, 1H, *J*=3.8 and *J*=1.2 Hz, 3''-H), 7.79 (dd, 1H, *J*=5.1 and *J*=1.2 Hz, 5''-H), 7.99–8.02 (m, 2H, 4-H and 7-H). ¹³C NMR (acetone-*d*₆) δ 11.4, 25.4, 46.6, 106.2, 116.3, 123.0 (2 overlapped signals), 124.4, 127.0, 127.2, 128.9, 129.1, 129.3, 132.9, 134.7, 138.6, 154.32, 178.5. λ_{max} (Dioxane)/nm 500 ($\epsilon/\text{dm}^3 \text{ mol}^{-1}$ 35,400). IR (CHCl₃): ν 2919, 1506, 1454, 1366, 1341, 1314, 1189, 1158, 1132, 1046, 838, 757, 728, 702 cm⁻¹. MS (microTOF) *m/z* (%)=353 ([M+H]⁺, 100), 352 (M⁺, 30), 323 (6), 255 (37). HMRS: *m/z* (MicroTOF) for C₁₈H₁₇N₄S₂; calcd; 353.09016; found: 353.08891.

4.2.4. 2-(Benzo[d]thiazol-2-yl)-1-(1-(4-methoxyphenyl)-5-(thiophen-2-yl)-1H-pyrrol-2-yl)-diazene 5b. Violet solid (58 mg, 27%). Mp 161–162 °C. ¹H NMR (acetone-*d*₆) δ 3.99 (s, 3H, OCH₃), 7.08–7.14 (m, 1H, 4'-H), 7.13 (d, 1H, *J*=4.9 Hz, 4'-H), 7.21 (dd, 2H, *J*=9.2 Hz, 3'''-H and 5'''-H), 7.27 (d, 1H, *J*=4.9 Hz, 3'-H), 7.29 (dd, 1H, *J*=3.6 and *J*=1.2 Hz, 3''-H), 7.40 (dt, 1H, *J*=7.6 and *J*=1.2 Hz, 5-H), 7.45–7.54 (m, 4H, 6-H, 3''-H, 2'''-H and 6'''-H), 7.56 (dd, 1H, *J*=5.3 and *J*=1.2 Hz,

5''-H), 7.90 (dd, 1H, *J*=8.4 and *J*=0.8 Hz, 4-H), 7.96 (dd, 1H, *J*=8.4 and *J*=0.8 Hz, 7-H). ¹³C NMR (DMSO) δ 55.5, 106.5, 114.5, 114.8, 122.4, 123.1, 126.0, 126.4, 127.7, 127.8, 128.8, 129.8, 130.7, 131.7, 133.2, 139.9, 148.9, 152.6, 160.1, 177.2. λ_{max} (Dioxane)/nm 509 ($\epsilon/\text{dm}^3 \text{ mol}^{-1}$ 35,780). IR (CHCl₃): ν 2926, 1512, 1456, 1341, 1324, 1314, 1249, 1222, 1196, 1180, 1166, 1045, 1002, 826, 759, 703 cm⁻¹. MS (microTOF) *m/z* (%): 417 ([M+H]⁺, 100), 416 (M⁺, 36), 391 (10), 296 (10), 247 (15), 225 (20). HMRS: *m/z* (MicroTOF) for C₂₂H₁₇N₄OS₂; calcd 417.0844; found: 417.0835.

4.2.5. 2-(Benzo[d]thiazol-2-yl)-1-(1-(4-fluorophenyl)-5-(thiophen-2-yl)-1H-pyrrol-2-yl)-diazene 5c. Violet solid (52 mg, 25%). Mp 199–200 °C. ¹H NMR (acetone-*d*₆) δ 7.10–7.13 (m, 1H, 4'-H), 7.13 (d, 1H, *J*=4.8 Hz, 4'-H), 7.27–7.29 (m, 2H, 3'-H, 3''-H), 7.41 (dt, 1H, *J*=7.6 and *J*=1.2 Hz, 5-H), 7.45–7.52 (m, 3H, 6-H, 3'''-H and 5'''-H), 7.59 (dd, 1H, *J*=5.2 and *J*=1.2 Hz, 5''-H), 7.65 (dd, 2H, *J*=8.8 and *J*=4.8 Hz, 2'''-H and 6'''-H), 7.90 (br d, 1H, *J*=7.9 Hz 4-H), 7.96 (br d, 1H, *J*=7.9 Hz, 7-H). ¹³C NMR (acetone-*d*₆) δ 115.1, 116.9, and 117.1 (d, *J*=20 Hz, C3'' and C5''), 122.9, 124.4, 127.0, 127.1, 128.6, 128.9, 129.3, 132.6, and 132.7, (d, *J*=8 Hz, C2'' and C6''), 133.0, 133.2, 134.8, 139.8, 149.8, 154.2, 162.8, and 165.3 (d, *J*=245 Hz, C4'') 178.4. λ_{max} (Dioxane)/nm 507 ($\epsilon/\text{dm}^3 \text{ mol}^{-1}$ 42,800). IR (CHCl₃): ν 3073, 2925, 1603, 1509, 1457, 1438, 1394, 1349, 1330, 1315, 1248, 1221, 1184, 1158, 1126, 1091, 1050, 1025, 1010, 884, 840, 815, 767, 755 cm⁻¹. MS (microTOF) *m/z* (%): 405 ([M+H]⁺, 100), 295 (17). HMRS: *m/z* (MicroTOF) for C₂₁H₁₄FN₄S₂; calcd 405.06384; found: 405.06372.

4.2.6. 2-(Benzo[d]thiazol-2-yl)-1-(1-(naphthalen-1-yl)-5-(thiophen-2-yl)-1H-pyrrol-2-yl)-diazene 5d. Dark red solid (68 mg, 30%). Mp 190–191 °C. ¹H NMR (acetone-*d*₆) δ 6.96–6.98 (m, 1H, 4'-H), 7.25 (dd, 1H, *J*=4.4 and *J*=1.2 Hz, 3''-H), 7.32–7.34 (m, 3H, 4'-H, and 2× Naphthyl-H), 7.40–7.43 (m, 3H, 3'-H, 5'-H, and Naphthyl-H), 7.51 (dt, 1H, *J*=7.8 and *J*=1.2 Hz, 5-H), 7.61 (dt, 1H, *J*=7.8 and *J*=1.2 Hz, 6-H), 7.84 (dd, 1H, *J*=8.0 and *J*=1.6 Hz, 4-H), 7.83–7.86 (m, 2H, 2× Naphthyl-H), 7.90 (dd, 1H, *J*=8.0 and *J*=1.6 Hz, 7-H), 8.18 (br d, *J*=8.4 Hz, 8'''-H), 8.31–8.35 (m, 1H, 2'''-H). ¹³C NMR (acetone-*d*₆) δ 106.9, 114.9, 122.8, 123.1, 124.3, 126.4, 126.9, 127.0, 127.7, 128.3, 128.5, 128.7, 129.1, 129.2, 129.3, 131.3, 132.7, 132.9, 133.6, 134.7, 135.2, 140.6, 150.3, 154.1, 178.2. λ_{max} (Dioxane)/nm 508 ($\epsilon/\text{dm}^3 \text{ mol}^{-1}$ 28,320). IR (CHCl₃): ν 3409, 2924, 2854, 1505, 1455, 1342, 1311, 1260, 1208, 1171, 1110, 1045, 840, 803, 774, 758 cm⁻¹. MS (microTOF) *m/z* (%): 437 ([M+H]⁺, 100), 436 (M⁺, 27), 380 (15), 378 (16), 359 (15), 318 (7), 247 (10), 225 (28). HMRS: *m/z* (MicroTOF) for C₂₅H₁₇N₄S₂; calcd 437.0895; found: 437.09040.

4.2.7. 2-(6-Methylbenzo[d]thiazol-2-yl)-1-(1-(propyl)-5-(thiophen-2-yl)-1H-pyrrol-2-yl)-diazene 6a. Violet solid (34 mg, 18%). Mp 120–121 °C. ¹H NMR (acetone-*d*₆) δ 1.03 (t, *J*=7.0 Hz, 3H, CH₃), 1.92–1.96 (m, 2H, CH₂), 2.86 (br s, 3H, Ph-CH₃), 4.61 (t, *J*=7.0 Hz, 2H, NCH₂), 6.87 (d, 1H, *J*=4.6 Hz, 4'-H), 7.12 (d, 1H, *J*=4.6 Hz, 3'-H), 7.32 (dd, *J*=5.2 and *J*=3.7, 1H, 4''-H), 7.35 (dd, 1H, *J*=8.3 and *J*=2 Hz, 5-H), 7.59 (br d, 1H, *J*=3.7 Hz, 3''-H), 7.79 (d, 1H, *J*=2 Hz, 7-H), 7.80 (dd, 1H, *J*=3.7 and 1.0 Hz, 5''-H), 7.88 (d, 1H, *J*=8.3 Hz, 4H). ¹³C NMR (acetone-*d*₆) δ 11.4, 21.6, 25.4, 46.5, 106.1, 116.1, 122.7, 124.1, 128.7, 128.8, 128.9, 129.3, 133.0, 134.9, 137.5, 138.1, 147.9, 152.4, 177.6. λ_{max} (Dioxane)/nm 503 ($\epsilon/\text{dm}^3 \text{ mol}^{-1}$ 30,060). IR (CHCl₃): ν 3851, 3646, 2925, 1731, 1597, 1505, 1455, 1436, 1413, 1342, 1311, 1260, 1230, 1208, 1186, 1171, 1110, 1045, 1017, 969, 841, 803, 774, 759, 727 cm⁻¹. MS (microTOF) *m/z* (%): 366 ([M]⁺, 18), 338 (20), 309 (18), 296 (30), 206 (40), 164 (80), 163 (100), 136 (18), 121 (35), 110 (21), 97 (31). HMRS: *m/z* (MicroTOF) for C₁₉H₁₈N₄S₂; calcd 366.0973; found: 366.0989.

4.2.8. 2-(Benzo[d]thiazol-6-yl)-1-(1-(propyl)-5-(thiophen-2-yl)-1H-pyrrol-2-yl)-diazene 7a. Orange solid (148 mg, 81%). Mp 105–107 °C. ¹H NMR (acetone-*d*₆) δ 0.93 (t, 3H, *J*=7.5 Hz, CH₃),

1.80–1.92 (m, 2H, CH₂), 4.58 (t, 2H, *J*=7.5 Hz, NCH₂), 6.58 (d, 1H, *J*=4.7 Hz, 4'-H), 6.83 (d, 1H, *J*=4.7 Hz, 3'-H), 7.19–7.22 (m, 1H, 4''-H), 7.35 (dd, 1H, *J*=3.5 and 1.2 Hz, 3''-H), 7.59 (dd, 1H, *J*=5.0 and 1.2 Hz, 5''-H), 8.06 (dd, 1H, *J*=8.7 and 1.8 Hz, 5-H), 8.18 (d, 1H, *J*=8.7 Hz, 4-H), 8.53 (d, 1H, *J*=1.8 Hz, 7-H). 9.30 (s, 1H, 2-H). ¹³C NMR (acetone-*d*₆) δ 11.4, 25.5, 46.0, 101.2, 113.3, 117.1, 120.6, 124.4, 127.1, 127.2, 128.7, 132.9, 134.1, 135.8, 148.3, 152.2, 154.8, 156.9. λ_{max}(Dioxane)/nm 451 (ε/dm³ mol⁻¹ cm⁻¹ 26,800). IR (CHCl₃): ν 3103, 3071, 2963, 2931, 2873, 1790, 1693, 1593, 1546, 1537, 1501, 1463, 1432, 1403, 1366, 1343, 1328, 1293, 1247, 1224, 1207, 1178, 1142, 1116, 1081, 1035, 955, 936, 912, 844 cm⁻¹. MS (EI-TOF) *m/z* (%)=352 ([M]⁺, 75), 206 (30), 203 (69), 191 (100), 177 (53), 163 (50), 134 (52), 121 (68). HMRS: *m/z* (MicroTOF) for C₁₈H₁₆N₄S₂; calcd 352.0816; found: 352.0807.

4.2.9. 2-(Benzo[d]thiazol-6-yl)-1-(1-(4-methoxyphenyl)-5-(thiophen-2-yl)-1H-pyrrol-2-yl)-diazene **7b**. Orange solid (175 mg, 81%). Mp 172–174 °C. ¹H NMR (acetone-*d*₆) δ 3.96 (s, 3H, OCH₃), 6.87 (d, 1H, *J*=4.4 Hz, 4'-H), 7.00–7.02 (m, 3H, 3'-H, 3''-H, and 4''-H), 7.16 (d, 2H, *J*=8.0 Hz, 3'''-H and 5'''-H), 7.42–7.46 (m, 3H, 5''-H, 2'''-H, and 6'''-H), 7.76 (dd, 1H, *J*=8.8 and *J*=2.1 Hz, 5-H), 8.07 (dd, 1H, *J*=8.8 Hz, 4-H), 8.33 (d, 1H, *J*=2.1 Hz, 7-H), 9.31 (s, 1H, 2-H). ¹³C NMR (acetone-*d*₆) δ 55.9, 101.5, 112.4, 115.0, 117.6, 120.1, 124.4, 126.8, 127.2, 128.2, 130.4, 131.5, 134.4, 135.3, 135.7, 150.3, 152.1, 154.9, 157.1, 161.1. λ_{max}(Dioxane)/nm 461 (ε/dm³ mol⁻¹ cm⁻¹ 21,900). IR (CHCl₃): ν 2955, 2924, 2854, 1515, 1462, 1378, 1297, 1251, 1206, 1168, 1035, 1018, 872, 836, 779, 722 cm⁻¹. MS (EI-TOF) *m/z* (%): 416 ([M]⁺, 100), 373 (16), 270 (97), 255 (40), 210 (18), 134 (21), 121 (77). HMRS: *m/z* (EI-TOF) for C₂₂H₁₆N₄O₂S₂; calcd 416.0766; found: 416.0782.

4.2.10. 2-(Benzo[d]thiazol-6-yl)-1-(1-(4-fluorophenyl)-5-(thiophen-2-yl)-1H-pyrrol-2-yl)-diazene **7c**. Orange solid (49 mg, 30%). Mp 191–192 °C. ¹H NMR (acetone-*d*₆) δ 6.87 (d, 1H, *J*=4.5 Hz, 4'-H), 7.00 (d, 1H, *J*=4.5 Hz, 3'-H), 7.00–7.04 (m, 2H, 3''-H and 4''-H), 7.41 (t, 2H, *J*=8.8 Hz, 3'''-H and 5'''-H), 7.45 (dd, 1H, *J*=5.1 and *J*=1.2 Hz, 5''-H), 7.61 (dd, 2H, *J*=8.8 and 4.8 Hz, 2'''-H and 6'''-H), 7.76 (dd, 1H, *J*=8.8 and *J*=2.0 Hz, 5-H), 8.08 (d, 1H, *J*=9.2 Hz, 4-H), 8.34 (d, 1H, *J*=1.6 Hz, 7-H). 9.31 (s, 1H, 2-H). ¹³C NMR (acetone-*d*₆) δ 101.4, 112.6, 112.6, and 116.8 (d, *J*=23 Hz, C3''' and C5'''), 117.7, 120.2, 124.4, 127.0, 127.2, 128.3, 132.5, and 132.6 (d, *J*=9 Hz, C2''' and C6'''), 134.1, 134.20, 134.23, 134.8, 135.8, 150.1, 152.2, 155.1, 157.2, 162.4, and 164.9 (d, *J*=245 Hz, C4'''). λ_{max}(Dioxane)/nm 452 (ε/dm³ mol⁻¹ cm⁻¹ 36,130). IR (CHCl₃): ν 3062, 2354, 1522, 1463, 1434, 1383, 1330, 844, 836, 783, 698 cm⁻¹. Anal. Calcd for C₂₁H₁₃FN₄S₂: C, 62.36, H, 3.24, N, 13.85. Found: C, 62.04, H, 3.30, N, 13.46.

4.3. Instruments

NMR spectra were obtained on a Varian Unity Plus Spectrometer at an operating frequency of 300 MHz for ¹H NMR and 75.4 MHz for ¹³C NMR or a Bruker Avance III 400 at an operating frequency of 400 MHz for ¹H NMR and 100.6 MHz for ¹³C NMR using the solvent peak as internal reference at 25 °C. All chemical shifts are given in parts per million using δ_H Me₄Si=0 ppm as reference and *J* values are given in hertz. Assignments were made by comparison of chemical shifts, peak multiplicities and *J* values and were supported by spin decoupling-double resonance and bidimensional heteronuclear HMBC and HMQC correlation techniques. IR spectra were determined on a BOMEM MB 104 spectrophotometer using KBr discs. UV–vis absorption spectra (200–800 nm) were obtained using a Shimadzu UV/2501PC spectrophotometer. Mass spectrometry analyses were performed at the 'C.A.C.T.I.-Unidad de Espectrometría de Masas' at the University of Vigo, Spain. Thermogravimetric analysis of samples was carried out using a TGA instrument model Q500 from TA Instruments, under high purity nitrogen supplied at a constant 50 mL min⁻¹ flow rate. All samples were subjected to a 20 °C min⁻¹ heating rate and were characterized between 25 and

500 °C. All melting points were measured on a Gallenkamp melting point apparatus and are uncorrected. Cyclic voltammetry (CV) was performed using a potentiostat/galvanostat (AUTOLAB/PSTAT 12) with the low current module ECD from ECO-CHEMIE and the data analysis processed by the General Purpose Electrochemical System software package also from ECO-CHEMIE. Three electrode-two compartment cells equipped with vitreous carbon-disc working electrodes, a platinum-wire secondary electrode and a silver-wire pseudo-reference electrode were employed for cyclic voltammetric measurements. The concentration of the compounds were 1 mmol dm⁻³ and 0.1 mol dm⁻³ [NBu₄][BF₄] was used as the supporting electrolyte in dry *N,N*-dimethylformamide solvent. The cyclic voltammetry was conducted usually at 0.1 V s⁻¹, or at different scan rates (0.02–0.50 V s⁻¹), for investigation of scan rate influence. The potential is measured with respect to ferrocenium/ferrocene as an internal standard.

4.4. Solvatochromic study

The solvatochromic study was performed using 10⁻⁴ mol dm⁻³ solutions of dyes **5–7** in several solvents at room temperature using a Shimadzu UV/2501PC spectrophotometer.

4.5. Nonlinear optical measurements using the Hyper-Rayleigh scattering (HRS) method

Hyper-Rayleigh scattering (HRS) was used to measure the first hyperpolarizability β of response of the molecules studied. The experimental set-up for Hyper-Rayleigh measurements employed a q-switched Nd:YAG laser and is similar to the one presented by Clays and Persoons.¹⁸ Details of the experimental procedure used have been previously published.^{15a} We emphasize that particular care was taken to avoid reporting artificially high first hyperpolarizabilities by using a pair of interference filters to estimate and correct for the presence of a possible contamination of the Hyper-Rayleigh signal by molecular fluorescence near 532 nm. Further cautions include normalizing the Hyper-Rayleigh signal at each pulse using the second harmonic signal from a 1 mm quartz plate to compensate for fluctuations in the temporal profile of the laser pulses due to longitudinal mode beating and the filtering of the solutions, using a 0.2 μm porosity filter, to avoid spurious signals from suspended impurities.

Dioxane was used as a solvent for all measurements. The small Hyper-Rayleigh signal that arises from dioxane was taken into account according to the expression

$$I_{2\omega} = G \left(N_{\text{solvent}} \langle \beta_{\text{solvent}}^2 \rangle + N_{\text{solute}} \langle \beta_{\text{solute}}^2 \rangle \right) I_{\omega}^2$$

where the factor *G* is an instrumental factor that takes into account the detection efficiency (including geometrical factors and linear absorption or scattering of the second harmonic light on its way to the detector) and local field corrections. The concentrations of the solutions under study were chosen so that the corresponding Hyper-Rayleigh signals fell well within the dynamic range of detection system. We have assumed that molecules could be treated as linear donor–acceptor chromophores with a first hyperpolarizability tensor dominated by a single longitudinal element, β₃₃₃=β, associated with the charge transfer axis. In this case the measured Hyper-Rayleigh signal is related to the value of the dominant tensor element through the relation $\beta = \sqrt{\langle \beta_{\text{HRS}}^2 \rangle} = \sqrt{\langle \beta_{\text{ZZZ}}^2 \rangle + \langle \beta_{\text{XZZ}}^2 \rangle}$ where the angle brackets denote an average for the random molecular orientations in the solution. Here we have adopted a laboratory reference frame in which the incident fundamental light propagates along the *X* axis and was vertically polarized along the *Z* direction, while no polarization discrimination was carried out

in the detection arm, which is orientated along the laboratory frame Yaxis. To calibrate our system a reference solution of *p*-nitroaniline (pNA) dissolved in dioxane at a concentration of 1×10^{-2} mol dm⁻³ (external reference method). Kaatz and Shelton^{19a} have measured the value of β_{333} of pNA in dioxane at 1064 nm to be 40×10^{-30} esu using the so-called Taylor convention for the first hyperpolarizability.^{19b} This value has been corrected by a factor of 1.88 for the most recent calibration factor of the Hyper-Rayleigh scattering signal of CCl₄, which was used as a reference.²³

Acknowledgements

Thanks are due to the Fundação para a Ciência e Tecnologia (Portugal) and FEDER for financial support through the Centro de Química and Centro de Física- Universidade do Minho, Project PTDC/QUI/66251/2006 (FCOMP-01-0124-FEDER-007429), Project PTDC/CTM/105597/2008 with funding from COMPETE/FEDER and a research grant to M. C. R. Castro (UMINHO/BI/142/2009). The NMR spectrometer Bruker Avance III 400 is part of the National NMR Network and was purchased within the framework of the National Program for Scientific Re-equipment, contract REDE/1517/RMN/2005 with funds from POCI 2010 (FEDER) and FCT.

We acknowledge the computational support of the Project SeARCH (Services and Advanced Research Computing with HTC/HPC clusters), funded by FCT under contract CONC-REEQ/443/EEI/2005.

Supplementary data

Supplementary data associated with this article can be found in the online version, at [doi:10.1016/j.tet.2011.05.053](https://doi.org/10.1016/j.tet.2011.05.053). These data include MOL files and InChIKeys of the most important compounds described in this article.

References and notes

- (a) Facchetti, A.; Abboto, A.; Beverina, L.; van der Boom, M. E.; Dutta, P.; Evmenenko, G.; Marks, T. J.; Pagani, G. A. *Chem. Mater.* **2002**, *14*, 4996; (b) Audibert, P.; Kamada, K.; Matsunaga, K.; Ohta, K. *Chem. Phys. Lett.* **2003**, *367*, 62; (c) Trofimov, B. A.; Markova, M. V.; Morozova, L. V.; Schmidt, E. Y.; Senotrusova, E. Y.; Myachina, G. F.; Myachin, Y. A.; Vakul'skaya, T. I.; Mikhaleva, A. I. *Polym. Sci. B* **2007**, *49*, 292; (d) Schmidt, E. Y.; Ushakov, I. A.; Zorina, N. V.; Mikhaleva, A. I.; Trofimov, B. A. *Mendeleev Commun.* **2011**, *21*, 36 and references cited therein.
- (a) Towns, A. D. *Dyes Pigments* **1999**, *42*, 3; (b) Yesodha, S. K.; Pillai, C. K. S.; Tsutsumi, N. *Prog. Polym. Sci.* **2004**, *29*, 45; (c) Astrand, P.-O.; Sommer-Larsen, P.; Hvilsted, S.; Ramanujam, P. S.; Bak, K. L.; Sauer, S. P. A. *Chem. Phys. Lett.* **2000**, *325*, 115; (d) Wang, Y.; Ma, J.; Jiang, Y. J. *Phys. Chem. A* **2005**, *109*, 7197; (e) Yager, K. G.; Barrett, C. J. *J. Photochem. Photobiol., A* **2006**, *182*, 250; (f) Nabeshima, Y.; Shishido, A.; Kanazawa, A.; Shiono, T.; Ikeda, T.; Hiyama, T. *Chem. Mater.* **1997**, *9*, 1480; (g) Zhu, Z.; Wan, Y.; Lu, Y. *Macromolecules* **2003**, *36*, 9585.
- For some recent examples in pyrrole azo dyes see: (a) Mikroyannidis, J. A.; Sharma, G. D.; Sharma, S. S.; Vijay, Y. K. *J. Phys. Chem. C* **2010**, *114*, 1520; (b) Mikroyannidis, J. A.; Roy, M. S.; Sharma, G. D. *J. Power Sources* **2010**, *195*, 5391; (c) Mikroyannidis, J. A.; Tsagkournos, D. V.; Sharma, S. S.; Kumar, A.; Vijay, Y. K.; Sharma, G. D. *Sol. Energy Mater. Sol. Cells* **2010**, *94*, 2318.
- For some recent examples in pyrrole azo dyes see: (a) Mohr, G. J.; Nezel, T.; Spichiger, U. E. *Anal. Chim. Acta* **2000**, *414*, 181; (b) DiCesare, N.; Lakowicz, R. C. *Org. Lett.* **2001**, *3*, 3891; (c) Mohr, G. J. *Chem. Commun.* **2002**, 2646; (d) Wagner-Wysieka, E.; Luboch, E.; Kowalczyk, M.; Biernat, J. F. *Tetrahedron* **2003**, *59*, 4415; (e) Gunnlaugsson, T. J.; Leonard, P.; Murray, N. S. *Org. Lett.* **2004**, *6*, 1557; (f) Zhang, D.; Zhang, M.; Liu, Z.; Yu, M.; Li, F.; Yi, T.; Huang, C. *Tetrahedron Lett.* **2006**, *47*, 7093; (g) Trofimov, B. A.; Schmidt, E. Y.; Mikhaleva, A. I.; Vasiltsov, A. M.; Zaitsev, A. B.; Smolyanina, N. S.; Senotrusova, E. Y.; Afonin, A. V.; Ushakov, I. A.; Petrusenko, K. B.; Kazheva, O. N.; Dyachenko, O. A.; Smirnov, V. V.; Schmidt, A. F.; Markova, M. V.; Morozova, L. *Eur. J. Org. Chem.* **2006**, 4021; (h) Cheng, Y.-F.; Liu, Z.-Q.; Shi, M.; Zhao, Q.; Li, F.-Y.; Yi, T.; Huang, C.-H. *Chin. J. Chem.* **2007**, *25*, 616.
- (a) Dirk, C. W.; Katz, H. E.; Schilling, M. L.; King, L. A. *Chem. Mater.* **1990**, *2*, 700; (b) Miller, R. D.; Lee, V. Y.; Moylan, C. R. *Chem. Mater.* **1994**, *6*, 1023; (c) Rao, V. P.; Jen, A.-Y.; Wong, K. Y.; Drost, K. J. *Tetrahedron Lett.* **1993**, *34*, 1747.
- (a) Varanasi, P. R.; Jen, A.-Y.; Chandrasekar, J.; Nambhothiri, I. N. N.; Rathna, A. *J. Am. Chem. Soc.* **1996**, *118*, 12443; (b) Albert, I. D. L.; Marks, T. J.; Ratner, M. A. *J. Am. Chem. Soc.* **1997**, *119*, 6575; (c) Breitung, E. M.; Shu, C.-F.; McMahon, R. J. *J. Am. Chem. Soc.* **2000**, *122*, 1154; (d) Gilchrist, T. L. *Heterocyclic Chemistry*; Wiley: New York, NY, 1985; (e) Shu, C.-F.; Wang, Y.-K. *J. Mater. Chem.* **1998**, *8*, 833.
- (a) *Comprehensive Heterocyclic Chemistry*; Katritzky, A. R.; Rees, C. W., Eds.; Pergamon: Oxford, 1984; (b) Bradamante, S.; Facchetti, A.; Pagani, G. A. *J. Phys. Org. Chem.* **1997**, *10*, 514; (c) Facchetti, A.; Abboto, A.; Beverina, L.; van der Boom, M. E.; Dutta, P.; Evmenenko, G.; Pagani, G. A.; Marks, T. J. *Chem. Mater.* **2003**, *15*, 1064; (d) Abboto, A.; Beverina, L.; Bradamante, S.; Facchetti, A.; Klein, C.; Pagani, G. A.; Redi-Abshiro, M.; Wortmann, R. *Chem.—Eur. J.* **2003**, *9*, 1991; (e) Abboto, A.; Beverina, L.; Bradamante, S.; Facchetti, A.; Pagani, G. A.; Bozio, R.; Ferrante, C.; Pedron, D.; Signorini, R. *Synth. Met.* **2003**, *14*, 4996; (f) Facchetti, A.; Beverina, L.; van der Boom, M. E.; Dutta, P.; Evmenenko, G.; Pagani, G. A.; Marks, T. J. *J. Am. Chem. Soc.* **2006**, *128*, 2142; (g) Davies, J. A.; Elangovan, A.; Sullivan, P. A.; Olbricht, B. C.; Bale, D. H.; Ewy, T. R.; Isborn, C. M.; Eichinger, B. E.; Robinson, B. H.; Reid, P. J.; Li, X.; Dalton, L. R. *J. Am. Chem. Soc.* **2008**, *130*, 10565; (h) Abboto, A.; Beverina, L.; Manfredi, N.; Pagani, G. A.; Archetti, G.; Kuball, H. G.; Wittenburg, C.; Heck, J.; Holtmann, J. *Chem.—Eur. J.* **2009**, *15*, 6175.
- (a) Raposo, M. M. M.; Sousa, A. M. R. C.; Fonseca, A. M. C.; Kirsch, G. *Tetrahedron* **2005**, *61*, 8249; (b) Raposo, M. M. M.; Sousa, A. M. R. C.; Kirsch, G.; Ferreira, F.; Belsley, M.; Matos Gomes, E.; Fonseca, A. M. C. *Tetrahedron* **2005**, *61*, 11991; (c) Raposo, M. M. M.; Sousa, A. M. R. C.; Kirsch, G.; Cardoso, P.; Belsley, M.; Matos Gomes, E.; Fonseca, A. M. C. *Org. Lett.* **2006**, *8*, 3681; (d) Batista, R. M. F.; Costa, S. P. G.; Malheiro, E. L.; Belsley, M.; Raposo, M. M. M. *Tetrahedron* **2007**, *63*, 4258; (e) Batista, R. M. F.; Costa, S. P. G.; Belsley, M.; Raposo, M. M. M. *Tetrahedron* **2007**, *63*, 9842; (f) Pina, J.; Seixas de Melo, S.; Batista, R. M. F.; Costa, S. P. G.; Raposo, M. M. M. *Phys. Chem. Chem. Phys.* **2010**, *12*, 9719; (g) Raposo, M. M. M.; Fonseca, A. M. C.; Castro, M. C. R.; Belsley, M.; Cardoso, M. F. S.; Carvalho, L. M.; Coelho, P. J. *Dyes Pigments* **2011**, *91*, 62.
- For some recent examples see: (a) Batista, R. M. F.; Costa, S. P. G.; Raposo, M. M. M. *Tetrahedron Lett.* **2004**, *45*, 2825; (b) Lacroix, P. G.; Padilla-Martínez, I. I.; López, H. S.; Nakatani, K. *New J. Chem.* **2004**, *28*, 542; (c) Martínez-Rubio, M.; Velasco, D.; Brillias, E.; Julià, L. *Tetrahedron* **2004**, *60*, 285; (d) Hrobárik, P.; Zahradník, P.; Fabian, W. M. F. *Phys. Chem. Chem. Phys.* **2004**, *6*, 495; (e) López-Calahorra, F.; Molinos-Gómez, A.; Vidal, X.; Maymó, M.; Velasco, D.; Martorell, J.; López-Calahorra, F. *Tetrahedron* **2005**, *61*, 9075; (f) Hrobárik, P.; Sigmundová, I.; Zahradník, P. *Synthesis* **2005**, 600; (g) Cui, Y.; Qian, G.; Chen, L.; Wang, Z.; Gao, J.; Wang, M. J. *Phys. Chem. B* **2006**, *110*, 4105; (h) Costa, S. P. G.; Batista, R. M. F.; Cardoso, P.; Belsley, M.; Raposo, M. M. M. *Eur. J. Org. Chem.* **2006**, *17*, 3938; (i) Coe, B. J.; Harris, J. A.; Hall, J. J.; Brunschwig, B. S.; Hung, S.-T.; Libaers, W.; Clays, K.; Coles, S. J.; Horton, P. N.; Light, M. E.; Hursthouse, M. B.; Garín, J.; Orduna, J. *Chem. Mater.* **2006**, *18*, 5907; (j) Hrobárik, P.; Sigmundová, I.; Zahradník, P.; Kasák, P.; Arion, V.; Franz, E.; Clays, K. *J. Phys. Chem. C* **2010**, *114*, 22289; (k) Razus, A. C.; Birzan, L.; Surugiu, N. M.; Corbu, A. C.; Chiraleu, F. *Dyes Pigments* **2007**, *74*, 26; (l) Chen, L.; Cui, Y.; Qian, G.; Wang, M. *Dyes Pigments* **2007**, *73*, 338; (m) Zajac, M.; Hrobárik, P.; Magdolen, P.; Foltínová, P.; Zahradník, P. *Tetrahedron* **2008**, *64*, 10605; (n) Quist, F.; Christophe, M. L.; Velde, V.; Didier, D.; Teshome, A.; Asselberghs, I.; Clays, K.; Sergeyev, S. *Dyes Pigments* **2009**, *81*, 203; (o) Coe, B. J.; Foxon, S. P.; Harper, E. C.; Harris, J. A.; Helliwell, M.; Raftery, J.; Asselberghs, I.; Clays, K.; Franz, E.; Brunschwig, B. S.; Fitch, A. G. *Dyes Pigments* **2009**, *82*, 171; (p) Hrobáriková, V.; Hrobárik, P.; Gajdoš, P.; Fitolis, I.; Fakis, M.; Persephonis, P.; Zahradník, P. *J. Org. Chem.* **2010**, *75*, 3053; (q) Andreu, R.; Galán, E.; Garín, J.; Orduna, J.; Alicante, R.; Villacampa, B. *Tetrahedron Lett.* **2010**, *51*, 6863.
- Coelho, P. J.; Carvalho, L. M.; Fonseca, A. M. C.; Raposo, M. M. M. *Tetrahedron Lett.* **2006**, *47*, 3711.
- (a) Raposo, M. M. M.; Sampaio, A. M. B. A.; Kirsch, G. *Synthesis* **2005**, 2, 199; (b) Raposo, M. M. M.; Sousa, A. M. R. C.; Fonseca, A. M. C.; Kirsch, G. *Tetrahedron* **2006**, *62*, 3493.
- (a) Abboto, A.; Bradamante, S.; Pagani, G. A. *J. Org. Chem.* **1996**, *61*, 1761; (b) Hrobárik, P.; Horváth, B.; Sigmundová, I.; Zahradník, P.; Malkina, O. L. *Magn. Reson. Chem.* **2007**, *45*, 942.
- (a) Ogura, K.; Yanay, H.; Miokawa, M.; Akazome, M. *Tetrahedron Lett.* **1999**, *40*, 8887; (b) Chen, Y.; Harrison, W. T. A.; Imrie, C. T.; Ryder, K. S. *J. Mater. Chem.* **2002**, *12*, 579.
- Dincer, H. A.; Sener, M. K.; Koca, A.; Gul, A.; Kocak, M. B. *Electrochim. Acta* **2008**, *53*, 3459.
- (a) Herbivo, C.; Comel, A.; Fonseca, A. M. C.; Kirsch, G.; Belsley, M.; Raposo, M. M. M. *Dyes Pigments* **2010**, *86*, 217; (b) O'Connor, M. J.; Yelle, R. B.; Linz, T. M.; Haley, M. M. C. R. *Chim.* **2009**, *12*, 385.
- (a) Kamlet, M. J.; Abboud, J.-L. M.; Abraham, M. H.; Taft, R. W. *J. Org. Chem.* **1983**, *48*, 2877; (b) Kamlet, M. J.; Abboud, J.-M.; Abraham, M. H.; Taft, R. W. *J. Am. Chem. Soc.* **1977**, *99*, 6027.
- See for example. (a) Bossard, G.; Knöpfle, P.; Prêtre, P.; Günter, P. *J. Appl. Phys.* **1992**, *71*, 1594; (b) Kim, O.-K.; Fort, A.; Barzoukas, M.; Blanchard-Desce, M.; Lehn, J.-M. *J. Mater. Chem.* **1999**, *9*, 2227 and references cited.
- (a) Clays, K.; Persoons, A. *Rev. Sci. Instrum.* **1992**, *63*, 3285; (b) Clays, K.; Persoons, A. *Phys. Rev. Lett.* **1991**, *66*, 2980.
- (a) Kaatz, P.; Shelton, D. P. *J. Chem. Phys.* **1996**, *105*, 3918; (b) Reis, H. J. *Chem. Phys.* **2006**, *125* ARTN 014506.
- (a) Oudar, J. L. *J. Chem. Phys.* **1977**, *67*, 446; (b) Oudar, J. L.; Chemla, D. S. *J. Chem. Phys.* **1977**, *66*, 2664; (c) Zyss, J.; Oudar, J. L. *Phys. Rev. A* **1982**, *26*, 2016.
- (a) Ra, C. S.; Kim, S. C.; Park, C. J. *Mol. Struct.-Theochem* **2004**, *677*, 173; (b) Nandi, P. K.; Panja, N.; Ghanty, T. K. *J. Phys. Chem. A* **2008**, *112*, 4844.
- Frisch, M. J.; Trucks, G. W.; Schlegel, H. B.; Scuseria, G. E.; Robb, M. A.; Cheeseman, J. R.; Scalmani, G.; Barone, V.; Mennucci, B.; Petersson, G. A.; Nakatsuji, H.; Caricato, M.; Li, X.; Hratchian, H. P.; Izmaylov, A. F.; Bloino, J.;

- Zheng, G.; Sonnenberg, J. L.; Hada, M.; Ehara, M.; Toyota, K.; Fukuda, R.; Hasegawa, J.; Ishida, M.; Nakajima, T.; Honda, Y.; Kitao, O.; Nakai, H.; Vreven, T.; Montgomery, J. A., Jr.; Peralta, J. E.; Ogliaro, F.; Bearpark, M.; Heyd, J. J.; Brothers, E.; Kudin, K. N.; Staroverov, V. N.; Kobayashi, R.; Normand, J.; Raghavachari, K.; Rendell, A.; Burant, J. C.; Iyengar, S. S.; Tomasi, J.; Cossi, M.; Rega, N.; Millam, N. J.; Klene, M.; Knox, J. E.; Cross, J. B.; Bakken, V.; Adamo, C.; Jaramillo, J.; Gomperts, R.; Stratmann, R. E.; Yazyev, O.; Austin, A. J.; Cammi, R.; Pomelli, C.; Ochterski, J. W.; Martin, R. L.; Morokuma, K.; Zakrzewski, V. G.; Voth, G. A.; Salvador, P.; Dannenberg, J. J.; Dapprich, S.; Daniels, A. D.; Farkas, Ö.; Foresman, J. B.; Ortiz, J. V.; Cioslowski, J.; Fox, D. J. *Gaussian 09, Revision A.1*; Gaussian: Wallingford CT, 2009.
23. Pyatt, R. D.; Shelton, D. P. *J. Chem. Phys.* **2001**, *114*, 9938.